

---

# JOURNAL OF THE AMERICAN CHEMICAL SOCIETY

---

## Paramagnetic NMR Spectroscopy of Microperoxidase-8

Donald W. Low,<sup>†</sup> Harry B. Gray,<sup>\*,†</sup> and Jens Ø. Duus<sup>\*,‡</sup>

Contribution from the Beckman Institute 139-74, California Institute of Technology, Pasadena, California 91125, and the Department of Chemistry, Carlsberg Laboratory, Gamle Carlsberg Vej 10, DK-2500, Valby, Denmark

Received August 22, 1996<sup>⊗</sup>

**Abstract:** Microperoxidase-8 (MP8) is the heme octapeptide derived from enzymatic proteolysis of horse-heart cytochrome *c*. Not only is MP8 a functional peroxidase (it catalyzes the oxidation of various substrates by hydrogen peroxide), it has also served as a useful calibration for the interpretation of the electronic spectroscopic properties of heme proteins. NMR structural characterization of MP8 has been difficult, owing to extensive aggregation at millimolar concentrations. We have obtained well-resolved <sup>1</sup>H and <sup>13</sup>C NMR spectra of monomeric ferric MP8-CN in mixed aqueous-organic solvent mixtures containing excess cyanide. Most peptide resonances were assigned by through-bond correlations using TOCSY spectra; heme resonances were identified largely by through-space correlations using NOESY spectra. HMQC spectra were interpreted with the aid of proton assignments to identify <sup>13</sup>C resonances. Most peptide resonances appear within the diamagnetic region and are very sharp, the exceptions being resonances associated with the His18 residue. Protons on the His18 imidazole ring exhibit very broad resonances, reflecting efficient relaxation. The signals of heme substituents are shifted outside of the diamagnetic envelope, with heme methyl resonances appearing between 10 and 25 ppm. The pattern of MP8-CN heme methyl resonances bears a striking resemblance to those of intact cyanoferric heme *c* protein derivatives. Large amide-proton/α-proton coupling constants and interresidue NOE contacts were found between residues 14 and 18, while moderate amide-α coupling constants were found between residues 19 and 21. The imidazole group of His18 remains coordinated to the ferric center in MP8; and the pattern of heme methyl resonances confirms that a fixed axial imidazole orientation is preserved in the isolated heme active site. The observed interresidue NOE's and amide-H/H<sub>α</sub> proton coupling constants indicate that His18 is part of a rigid loop of five residues anchored to the heme that serves to orient the axial imidazole, while residues 19-21 form a flexible C-terminal domain.

### Introduction

Microperoxidase-8 (MP8), the heme octapeptide derived from enzymatic cleavage of horse heart cytochrome *c* (h-cyt *c*), has been employed as a functional model for heme-containing enzymes.<sup>1</sup> The MP8 porphyrin is covalently attached to residues 14-21 of the protein (Cys Ala Gln Cys His Thr Val Glu) through thioether linkages at positions 14 and 17; in addition,

the imidazole of His18 binds axially to the iron, leaving the sixth coordination site to be occupied by exogenous ligands such as water or cyanide (Figure 1).<sup>2-7</sup> The resting state of MP8

<sup>†</sup> California Institute of Technology.

<sup>‡</sup> Carlsberg Laboratory.

<sup>⊗</sup> Abstract published in *Advance ACS Abstracts*, December 15, 1996.

(1) Adams, P. A.; Baldwin, D. A.; Marques, H. M. In *Cytochrome c: a multidisciplinary approach*; Scott, R. A., Mauk, A. G., Eds.; University Science Books: Sausalito, 1996; pp 635-692.

(2) Aron, J.; Baldwin, D. A.; Marques, H. M.; Pratt, J. M.; Adams, P. A. *J. Inorg. Biochem.* **1986**, *27*, 227-243.

(3) Blumenthal, D. C.; Kassner, R. J. *J. Biol. Chem.* **1980**, *255*, 5859-5863.

(4) Smith, M. C.; McLendon, G. *J. Am. Chem. Soc.* **1980**, *102*, 5666-5670.

(5) Wang, J.-S.; Tsai, A.-L.; Heldt, J.; Palmer, G.; Wart, H. E. V. *J. Biol. Chem.* **1992**, *267*, 15310-15318.

(6) Wang, J.-S.; Wart, H. E. V. *J. Phys. Chem.* **1989**, *93*, 7925-7931.

(7) Bushnell, G. W.; Louie, G. V.; Brayer, G. D. *J. Mol. Biol.* **1990**, *214*, 585-595.

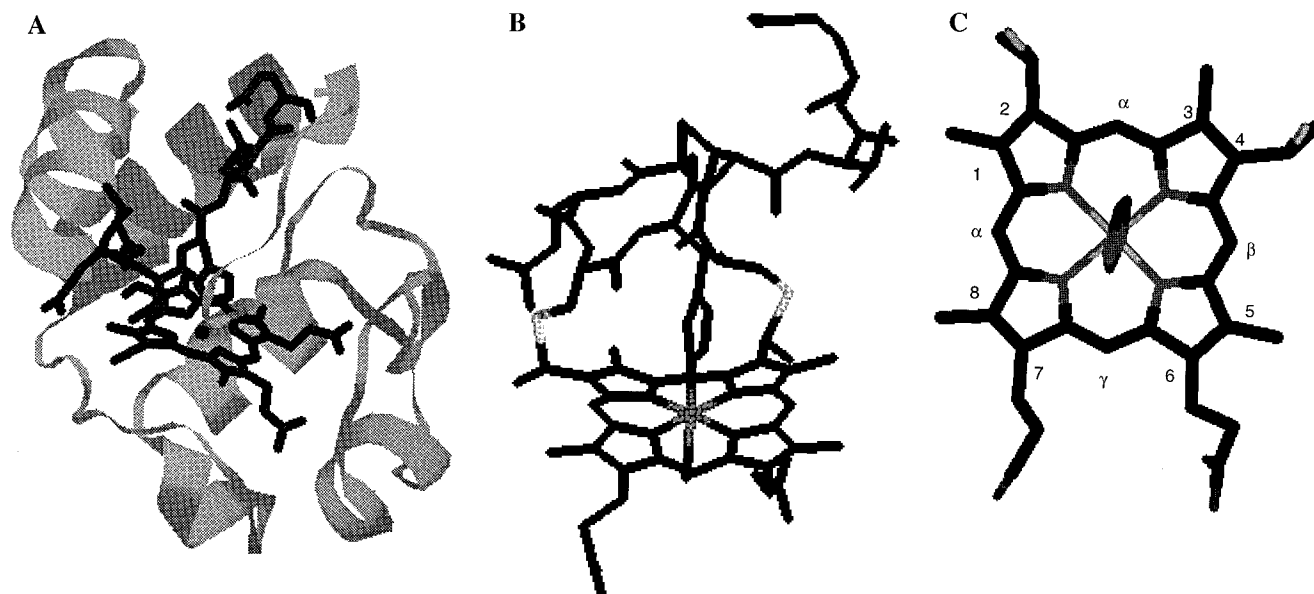


**Figure 1.** (A) Structure of h-cyt *c* with heme and residues 14–21 highlighted (coordinates from ref 7). (B) Fragment of h-cyt *c* structure corresponding to MP8. (C) Orientation of the His18 imidazole in h-cyt *c*.

features an exchangeable aquo or hydroxo ligand,<sup>2,8</sup> closely analogous to the active-site water in met myoglobin and Ala80 cytochrome *c*.<sup>9</sup> Microperoxidases have attracted attention not only as oxidation catalysts,<sup>10</sup> but also because of a growing number of sensor applications based on spectroscopic changes induced by exposure to hydrogen peroxide.<sup>11</sup>

The heme of MP8 has been characterized extensively by spectroscopic methods.<sup>5,6,12–16</sup> One method that potentially could reveal information about both the octapeptide conformation and the heme electronic structure is paramagnetic NMR spectroscopy.<sup>17–19</sup> However, the NMR spectra of MP8 in buffered aqueous solutions are very poorly resolved, owing to extensive aggregation and the presence of a high-spin iron center. These problems can be overcome by making measurements on the low-spin ferric-cyanide derivative<sup>3</sup> in methanolic solutions. Indeed, we have obtained highly resolved <sup>1</sup>H and <sup>13</sup>C NMR spectra of MP8 under these conditions. Analysis of the results suggests that the loop formed by residues 14–18 is extremely rigid and retains the gross structural features of the intact cytochrome, including a fixed axial ligand orientation.

## Results and Discussion

Addition of excess sodium cyanide to a brown methanolic solution of MP8 results in a deep red species whose electronic absorption (Soret  $\lambda_{\max}$  410 nm) and resonance Raman (441.6

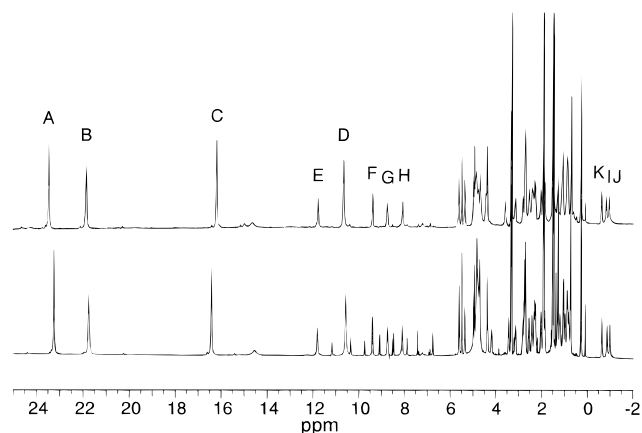


**Figure 2.** 250-MHz <sup>1</sup>H-NMR spectra of MP8-CN (5 mM MP8, 15 mM NaCN) in methanol-*d*<sub>4</sub> at 300 K before (upper spectrum) and after (lower spectrum) the addition of 10% H<sub>2</sub>O. Heme methyl resonances are labeled A–D; paramagnetically shifted His18 resonances are labeled E–G;  $\gamma$ ,  $\beta$ , and  $\delta$  meso proton resonances are labeled H, I, and J, respectively. Resonance K is due to the heme 4 $\alpha$  proton.

nm excitation,  $\nu_4 = 1373 \text{ cm}^{-1}$ ,  $\nu_3 = 1503 \text{ cm}^{-1}$ ,  $\nu_2 = 1585 \text{ cm}^{-1}$ ,  $\nu_{10} = 1642 \text{ cm}^{-1}$ ) properties are typical of a low-spin ( $S = 1/2$ ) heme.<sup>20</sup> The 250-MHz 1-D <sup>1</sup>H NMR spectrum of a 5 mM solution of MP8-CN in 90% MeOH-*d*<sub>4</sub>/10% H<sub>2</sub>O at 300 K is shown in Figure 2. Spectra taken of samples of MP8-CN in buffered aqueous solutions feature broad peaks that suggest extensive aggregation in solution, while spectra obtained from methanolic solutions have sharp spectral features, indicating minimal aggregation. The spectrum of MP8-CN features several peaks shifted well out of the diamagnetic envelope due to the effects of the paramagnetic ferric ion. The heme methyl substituents resonate between 10 and 25 ppm, a region typical for analogous  $S = 1/2$  met-cyano heme proteins.<sup>21</sup> The heme substituents are expected to exhibit only dipolar couplings to each other, and therefore NOESY spectroscopy was employed to assign their resonances (Table 1). A NOESY spectrum with a 200 ms mixing time features a self-consistent set of NOESY cross peaks, leading to an unambiguous assignment of the heme

(8) Munro, O. Q.; Marques, H. M. *Inorg. Chem.* **1996**, *35*, 3752–3767.

(9) Bren, K. L.; Gray, H. B. *J. Am. Chem. Soc.* **1993**, *115*, 10382–10383.

(10) Cunningham, I. D.; Bachelor, J. L.; Pratt, J. M. *J. Chem. Soc., Perkin Trans.* **1991**, *2*, 1839–1843.

(11) Tatsuma, T.; Watanabe, T. *Anal. Chem.* **1991**, *63*, 1580–1585.

(12) Silin, V. I.; Talaikyte, Z.; Kulys, J. *Vib. Spectrosc.* **1993**, *345*–351.

(13) Othman, S.; Lirzin, A. L.; Desbois, A. *Biochemistry* **1994**, *33*, 15437–15448; **1993**, *32*, 9781–9791.

(14) Kintner, E. T.; Dawson, J. H. *Inorg. Chem.* **1991**, *30*, 4892–4897.

(15) Kobayashi, N.; Osa, T. *Chem. Pharm. Bull.* **1989**, *37*, 3105–3107.

(16) Othman, S.; Lirzin, A. L.; Desbois, A. *Biochemistry* **1993**, *32*, 9781–9791.

(17) Bertini, I.; Turano, P.; Vila, A. J. *Chem. Rev.* **1993**, *93*, 2833–2932.

(18) Bertini, I.; Luchinat, C. *NMR of Paramagnetic Molecules in Biological Systems*; Benjamin/Cummings: Menlo Park, CA, 1986; p 319.

(19) Smith, M.; McLendon, G. *J. Am. Chem. Soc.* **1981**, *103*, 4912–4921. Mazumdar, S.; Mehdi, O. K.; Mitra, S. *Inorg. Chem.* **1991**, *30*, 700–705.

(20) Spiro, T. G. *Adv. Protein Chem.* **1985**, *17*, 111–159.

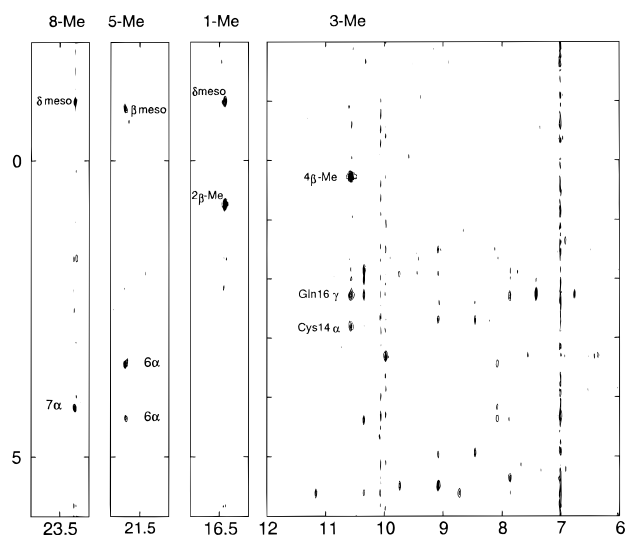
(21) Rajarathnam, K.; LaMar, G. N.; Chiu, M. L.; Sligar, S. G.; Singh, J. P.; Smith, K. M. *J. Am. Chem. Soc.* **1991**, *113*, 7886–7892.

**Table 1.**  $^1\text{H}$  Chemical Shifts

(A) Heme Substituents					
substituent	$\delta$ (ppm)	substituent	$\delta$ (ppm)	substituent	$\delta$ (ppm)
1-CH <sub>3</sub>	16.41	4 $\beta$ -CH <sub>3</sub>	0.27	$\gamma$ - meso	8.09
2 $\alpha$ -H	0.89	$\beta$ -meso	-0.86	7 $\alpha$ -CH <sub>2</sub>	4.20, 4.68
2 $\beta$ -CH <sub>3</sub>	0.74	5-CH <sub>3</sub>	21.73	7 $\beta$ -CH <sub>2</sub>	1.05, 1.20
$\alpha$ -meso	4.67	6 $\alpha$ -CH <sub>2</sub>	3.42, 4.36	8-CH <sub>3</sub>	23.24
3-CH <sub>3</sub>	10.57	6 $\beta$ -CH <sub>2</sub>	0.81, 0.91	$\delta$ -meso	-0.99
4 $\alpha$ -H	-0.63				

(B) Peptide Resonances (ppm)						
residue	amide	$\alpha$	$\beta_1$	$\beta_2$	$\gamma$	other
Cys14		2.82	2.71	3.12		
Ala15		5.61	1.90			
Gln16	10.36	4.39	1.85	2.01	2.28	6.76, 7.42
Cys17	7.87	5.36	1.05	2.31		
His18	11.16	9.39	8.72	11.80		
Thr19	9.74	5.49	4.98		1.91	
Val20	9.08	4.95	2.69		1.48	1.52
Glu21	8.46	4.71	2.42	2.54	2.72	

**Figure 3.** 600-MHz NOESY spectrum of MP8-CN in methanol- $d_4$  at 300 K (200 ms mixing time).

substituents (Figure 3). The 3-proton-intensity signals at 16.4 and 23.2 ppm both show a dipolar coupling to the upfield shifted 1-proton signal at -0.99 ppm, and are therefore assigned to the methyl groups at positions 1 and 8 and the  $\delta$ -meso proton, respectively. The methyl resonance at 21.7 ppm exhibits dipolar connectivities to a 1-proton signal at -0.86 ppm ( $\beta$ -meso) and methylene protons at 3.42 and 4.36 ppm, and therefore is assigned as the 5-CH<sub>3</sub>. The methyl resonance at 10.6 shows the dipolar connectivities expected for the 3-CH<sub>3</sub>, with cross peaks to a 1-proton singlet at 4.67 ppm ( $\alpha$ -meso) and to the 4 $\beta$ -CH<sub>3</sub>. The resonance at 23.2 ppm exhibits a NOESY cross peak to protons assigned to a propionate methylene unit, establishing its identity as the 8-CH<sub>3</sub>.

The observed pattern of heme substituent chemical shifts is very similar to those observed in the cyanide-bound forms of *Saccharomyces cerevisiae* Ala80 iso-1-cytochrome *c* (Ala80-y-cyt *c*), h-cyt *c*, and MP11 (Table 2). The methyl groups of MP8 resonate with a mean shift of 17.99 ppm and a spread of 12.3 ppm, compared with a mean shift of 17.1 ppm and a spread of 11.3 ppm for MP11, and a mean shift of 17.1 ppm and spread of 11.2 ppm for met-cyano Ala80-y-cyt *c*.<sup>22–24</sup> The chemical shift dispersion and mean chemical shift of the heme methyls are largely determined by the fixed orientations of the heme

**Table 2.** Comparison of Heme Methyl  $^1\text{H}$  Chemical Shifts<sup>a</sup>

	mean shift (ppm)	dispersion (ppm)
MP8-CN	17.99	12.3
MP11-CN	17.14	11.3
Ala80-y-cyt <i>c</i> -CN	17.10	11.2
ferric hemin-Im-CN	11.03	4.6

	methyl chemical shift (ppm)
MP8-CN	(8) 23.2; (5) 21.7; (1) 16.4; (3) 10.6
Ala80-y-cyt <i>c</i> -CN	(8) 22.5; (5) 19.5; (1) 15.4; (3) 11.3

<sup>a</sup>  $^1\text{H}$   $\delta$  values for MP11-CN, Ala80-y-cyt *c*-CN, and ferric hemin-Im-CN from refs 22–24.

axial ligands. Freely rotating or axially symmetric ligands result in relatively small values for mean shift and spread: ferric hemin imidazole cyanide has a spread of only 4.6 ppm and a mean methyl shift of 11.0 ppm.<sup>25</sup> After the replacement of methionine with an axially symmetric ligand such as cyanide, the imidazole orientation is then the primary factor in determining the rhombic axes. The similarity of the results for cyanide derivatives of MP8, Ala80-y-cyt *c*, and h-cyt *c* indicates a common fixed imidazole orientation in the heme *c* systems with the imidazole ring plane aligned with the  $\alpha$  and  $\gamma$  meso positions. Our finding that the gross orientation is preserved even in the absence of a large portion of the polypeptide chain, including Pro30, reported to provide a hydrogen bond to the imidazole,<sup>26</sup> suggests that the rigid loop of residues 14–18 fixes the orientation of the axial imidazole, modulating the distribution of heme spin density.

$^{13}\text{C}$  NMR spectroscopy has been employed to investigate paramagnetic heme systems.<sup>27–30</sup> Studies have focused on heme methyl chemical shifts, since, to a first approximation, dipolar contributions to their chemical shifts may be neglected and only the contact contribution from the iron need be considered. An HMQC spectrum of MP8-CN in methanol- $d_4$  is shown in Figure 4. The paramagnetic shifts felt by heme substituents in MP8 are paired: substituents on opposite sides of the porphyrin ring experience similar paramagnetic shifts (Figure 5). Turner has observed a similar phenomenon in the  $^{13}\text{C}$  spectra of ferricytochrome *c*<sub>3</sub>, in which axial imidazoles are found oriented along the  $\alpha$ – $\gamma$  meso axis.<sup>28</sup> An examination of the crystal structure of native cytochrome *c* reveals that the histidine in this case is also oriented along the  $\alpha$ – $\gamma$  meso axis;<sup>7</sup> and our data confirm that this orientation is preserved even in the MP8 active site.

All of the resonances from the peptide portion of MP8 except those of His18 fall within the diamagnetic region, and assignments were made with a combination of 2-D TOCSY and NOESY methods (Table 1B). Isolated spin systems were located in TOCSY spectra corresponding to each of the eight amino acid residues (Figure 6). In neat MeOH- $d_4$  solutions, no resonances are observed due to amide protons; however, upon addition of 10% H<sub>2</sub>O to methanolic solutions, 9 new resonances

(22) Kimura, K.; Peterson, J.; Wilson, M.; Cookson, D. J.; Williams, R. J. P. *J. Inorg. Biochem.* **1981**, *15*, 11–25.

(23) Satterlee, J. D. *Inorg. Chim. Acta* **1983**, *79*, 195–196.

(24) Bren, K. L.; Gray, H. B.; Banci, L.; Bertini, I.; Turano, P. *J. Am. Chem. Soc.* **1995**, *117*, 8067–8073.

(25) Traylor, T. G.; Berzini, A. P. *J. Am. Chem. Soc.* **1980**, *102*, 2844–2846.

(26) Moore, G. R.; Pettigrew, G. W. In *Cytochromes c*; Springer Verlag: New York, 1990; p 174.

(27) Santos, H.; Turner, D. L. *Eur. J. Biochem.* **1992**, *206*, 721–728.

(28) Turner, D. L.; Salgueiro, C. A.; Schenkels, P.; LeGall, J.; Xavier, A. V. *Biochim. Biophys. Acta* **1995**, *1246*, 24–28.

(29) Banci, L.; Bertini, I.; Pierattelli, R.; Vila, A. *J. Inorg. Chem.* **1994**, *33*, 4338–4343.

(30) Timkovich, R. *Inorg. Chem.* **1991**, *30*, 37–42.

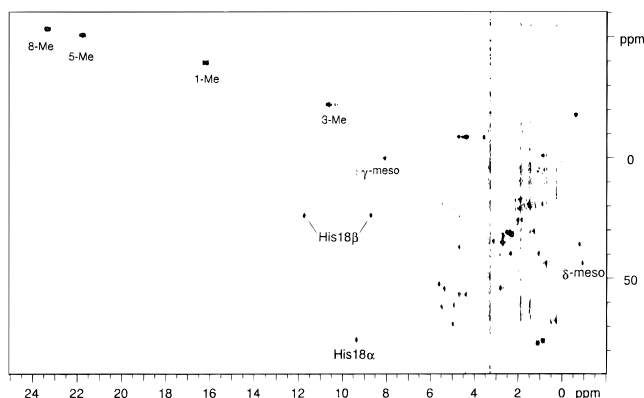


**Figure 4.** 600-MHz  $^1\text{H}$ - $^{13}\text{C}$  HMQC spectrum of 5 mM MP8-CN in methanol- $d_4$  at 300 K.

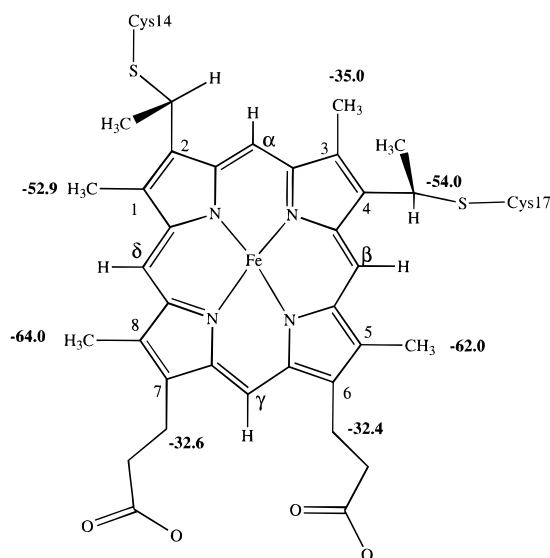


**Figure 5.** Estimated paramagnetic  $^{13}\text{C}$  chemical shifts of heme substituents.

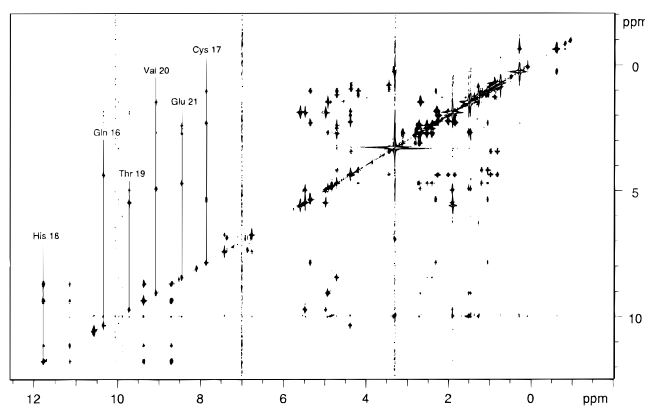


**Figure 6.** 600-MHz TOCSY spectrum of 5 mM MP8-CN in methanol- $d_4$  at 300 K (80 ms spinlock time, DIPSI spinlock).

are observed in the 5–10-ppm region where amide proton resonances are expected, and these are assigned to the amide protons of Cys14, Gln16, Cys17, His18, Thr19, Val20, and Glu21. Amide proton resonances from residues within the region of the peptide loop anchored to the heme show informative amide- $\alpha$   $J$  couplings: Cys17,  $^3J = 11$  Hz; Gln16,  $^3J = 4.7$  Hz; His18,  $^3J = 7.7$  Hz. For comparison, coupling constants were calculated using the Karplus relation;<sup>31</sup> torsional angles were taken from the crystal structure of h-cyt *c*.<sup>7</sup>

**Table 3.** Amide-H-H $\alpha$  Coupling Constants

residue	$\angle \text{NH-H}\alpha$ (deg) <sup>a</sup>	calcd $J_{\text{HH}'}$ (Hz) <sup>b</sup>	obsd $J_{\text{HH}'}$ (Hz)
Gln16	-124.4	4.7	4.7
Cys17	178.3	9.7	11.0
His18	143.0	7.1	7.6
Thr19	178.4	9.7	7.3
Val20	171.7	9.6	8.3
Glu21	-149.1	7.8	7.3

<sup>a</sup> From the crystal structure of h-cyt *c* (ref 7). <sup>b</sup> Calculated using the Karplus equation (ref 31) and H-N-C-H torsional angles obtained from the h-cyt *c* crystal structure (ref 7).

**Table 4.** Heme-Peptide NOE and Interresidue Contacts

(A) Heme-Peptide NOE Contacts		
heme substituent	peptide substituent	intensity classification <sup>b</sup>
2 $\alpha$	Cys14 $\alpha$	M
2 $\beta$	Cys14 $\alpha$	W
2 $\alpha$	Cys14 $\beta_1$	W <sup>a</sup>
$\alpha$ -meso	Cys14 $\alpha$	W <sup>a</sup>
3-CH <sub>3</sub>	Cys14 $\alpha$	M
3-CH <sub>3</sub>	Gln16 $\gamma$	M
3-CH <sub>3</sub>	Gln16 $\beta_2$	W
3-CH <sub>3</sub>	Gln16 NH	VW
4 $\alpha$	Cys17 $\beta_1$	M*
$\beta$ -meso	Cys17 $\beta_1$	VW
4 $\beta$	Cys17 $\beta$	VW
(B) Interresidue NOE Contacts		
peptide substituents		intensity classification
Cys14 $\beta_1$ -Ala15 $\alpha$ ,		W
Ala15 $\alpha$ -Gln16 NH,		W
Gln16 $\alpha$ -Cys17 NH,		W
Cys17 NH-His18 NH,		W
Thr19 $\alpha$ -Val20 NH,		S
Thr 19 $\beta$ -Val20 NH,		W
Val20 $\alpha$ -Glu21 NH,		W
Val20 $\beta$ -Glu21 NH,		VW
His18 $\beta_1$ -Ala15 $\beta$ ,		W
His18 $\beta_1$ -Ala15 $\alpha$ ,		M
His18 NH-Ala15 $\alpha$ ,		W
Cys17 NH-Ala15 $\alpha$ ,		W

<sup>a</sup> Correlation also found in Ala80-y-cyt *c* (ref 24). <sup>b</sup> VW = very weak, W = weak, M = moderate, S = strong.

Reasonable agreement between calculated and experimental  $J$  values was found for amide protons in the 14–18 loop, providing additional support for our finding that the structure of this loop in native cytochrome is retained in the peptide (Table 3). Dipolar couplings observed between heme thioether substituents are consistent with rigid conformations at heme positions 2 and 4: strong NOESY cross peaks are observed between the 2 $\beta$  CH<sub>3</sub> and the 1-CH<sub>3</sub> and a medium intensity cross peak is observed between the 2 $\alpha$  methine and the  $\alpha$ -meso protons. The 4 $\alpha$  methine proton shows a strong cross peak to the  $\beta$ -meso proton and the 4 $\beta$  CH<sub>3</sub> dipole couples strongly to the 3-CH<sub>3</sub>. Eleven interresidue NOESY cross peaks and eleven additional cross peaks between peptide and heme substituents were located and qualitatively classified in spectra taken in 90% MeOH- $d_4$ /10% H<sub>2</sub>O solutions (Table 4). NOESY spectra of Ala80-y-cyt *c* feature four cross peaks from heme pyrrole and meso substituents to peptide residues in the loop region.<sup>24</sup> Three of these involve cysteine  $\alpha$  and  $\beta$  protons on the peptide; these also appear in NOESY spectra of MP8-CN. The fourth contact involves the  $\epsilon$  and  $\gamma$  protons of Gln16, and its absence in spectra of MP8-CN is likely due to a change in the conformation of the flexible side chain. At least one sequential interresidue NOE was found to each of the amino acid residues except His18. Of

(31) Karplus, M. *J. Chem. Phys.* **1959**, *30*, 11–15.

the eleven interresidue NOE correlations found, eight arise from contacts within the Cys-Ala-Gln-Cys-His region, consistent with a rigid loop conformation. Two sets of resonances from Ala15 and His18 show NOE contacts across the 14–18 loop. Similar intermediate-range NOESY contacts are found between residues 15 and 18 of Ala80-y-cyt *c* and oxidized h-cyt *c*.<sup>32,33</sup> Outside the loop formed by residues 15–18, Val20 was found to have a large amide- $\alpha$  coupling, 8.7 Hz, and the other amide protons show couplings to neighboring  $\alpha$  protons of approximately 7 Hz, typical of fast rotational averaging on the NMR time scale, consistent with a more flexible C-terminal peptide domain.<sup>34</sup>

While the orientation of the methionine in native cytochrome *c* is believed to be the major determining factor in heme electronic asymmetry, recent work has shown that the fixed histidine orientation may also be important.<sup>28</sup> Heme electronic asymmetry could play a role in electron transfer by modulating the electronic coupling to the heme iron,<sup>35</sup> suggesting a functional role for imidazole orientation in these reactions. Immobilization of an axial ligand also will minimize changes in metal–ligand bond lengths and lower the inner-sphere reorganization energy associated with oxidation or reduction of the heme.<sup>36</sup> The heme and loop region 14–18 comprise a minimal heme active site that retains structural integrity even when isolated from its protein matrix, as reflected in the protein-like NMR spectroscopy of MP8. This rigid loop is highly conserved among *c* cytochromes and perhaps has evolved to orient the axial imidazole along the  $\alpha$ - $\gamma$  meso axis and modulate electron flow through the protein.

## Experimental Section

**Preparation of Ferric MP8-CN.** Microperoxidase-8 was prepared by peptic and tryptic digestion of h-cyt *c* (Sigma) and purified by reverse-phase FPLC as described previously.<sup>37</sup> A three-fold excess of solid sodium cyanide was added to NMR samples. Methanol-*d*<sub>4</sub> and D<sub>2</sub>O were used as received from Cambridge Isotopes.

**NMR Spectroscopy.** <sup>1</sup>H NMR experiments were performed at 250.13 (DRX 250) and 600.13 MHz (AMX 600) on Bruker instruments,

(32) Feng, Y.; Roder, H.; Englander, S. W.; Wand, A. J.; Stefano, D. L. *Biochemistry* **1989**, *28*, 195–203.

(33) Banci, L.; Bertini, I.; Bren, K. L.; Gray, H. B.; Somporpnisut, P.; Turano, P. *Biochemistry* **1995**, *34*, 11385–11398.

(34) Our results are consistent with a molecular modeling study of MP11 (Ranghino, G.; Antonini, G.; Fantucci, P. *Isr. J. Chem.* **1994**, *34*, 239–244) in which the C-terminal domain corresponding to residues 19–21 of MP8 is significantly more flexible than the 14–18 loop segment.

(35) Stuchebrukhov, A. A.; Marcus, R. A. *J. Phys. Chem.* **1995**, *99*, 7581–7590.

(36) Mayo, S. L.; Ellis, W. R.; Crutchley, R. J.; Gray, H. B. *Science* **1986**, *233*, 948–952.

(37) Low, D. W.; Winkler, J. R.; Gray, H. B. *J. Am. Chem. Soc.* **1996**, *118*, 117–120.

both with VTU2000 temperature control units; 1D<sup>13</sup>C spectra were obtained on an AM 500 spectrometer operating at 125.7 MHz. Accurate temperature control proved to be important for stability in 2D experiments, as several signals are very temperature sensitive. All experiments were done at 300 K. Assignments were made using Pronto software (Carlsberg) on Silicon Graphics Indigo workstations.<sup>38</sup> All experiments were performed with presaturation of the water signal by Gaussian-shaped selective pulses offset from the carrier frequency by phaseramps, using built-in Bruker software. One-dimensional <sup>1</sup>H spectra were acquired using sweep widths up to 20000 Hz at 600 MHz and 12500 Hz at 250 MHz. Two-dimensional <sup>1</sup>H spectra were obtained with sweep widths of 17850 Hz in both dimensions at 600 MHz, 4K points in F2, and 1K points in F1. The data were processed using standard Bruker software with zero filling to a final size of 2K × 2K complex points, and the data were multiplied by shifted squared sinebell windowfunctions prior to Fourier transform. NOESY spectra<sup>39</sup> were obtained with several mixing times from 50 to 300 ms, a presaturation time of 900 ms, and 32 to 48 scans per increment. TOCSY spectra were obtained using a DIPSI spinlock<sup>40</sup> with a spinlock power of 6000 Hz, a spinlock time of 80 ms, and 40 scans per increment. For both types of 2D spectra, quadrature detection in F1 was done by the Ruben–States–Haberkorn method.<sup>41</sup> Nonselective <sup>1</sup>H *T*<sub>1</sub> measurements<sup>42</sup> were made both at 250 and 600 MHz using the inversion–recovery method and 16 different delays from 100  $\mu$ s to 5 s, with a 5-s delay between scans. The data were analyzed using standard Bruker software with a 3-variable parameter fit. Estimates of *T*<sub>2</sub> relaxation times were made with a CPMG sequence<sup>43</sup> fitting the data to a single exponential decay. Assignments of <sup>13</sup>C data were based on 2D HMQC spectra measured both at 250 and 600 MHz. The sweep width in F1 was 42000 Hz at the 150.9 MHz resonance frequency for <sup>13</sup>C on the AMX600 and this was covered by 256 points using TPPI quadrature detection<sup>44</sup> and 420 scans per increment. The points were extended to 512 real points prior to Fourier transform by linear prediction and zero filled to a final size of 2K × 2K complex points.

**Acknowledgment.** We thank Ben Ramirez, Paola Turano, and Kara Bren for helpful discussions. This work was supported by NSF. D.W.L. acknowledges an award from the Parsons Foundation.

JA962948S

(38) Kjaer, M.; Andersen, K. V.; Poulsen, F. M. *Methods Enzymol.* **1994**, *239*, 288–307.

(39) Macura, S.; Ernst, R. R. *Mol. Phys.* **1980**, *41*, 95–117.

(40) Rucker, S. P.; Shaka, A. J. *Mol. Phys.* **1989**, *68*, 509–517.

(41) States, D. H.; Haberkorn, R. A.; Ruben, D. J. *J. Magn. Reson.* **1982**, *68*, 509–517.

(42) Vold, R. L.; Waugh, J. S.; Klein, M. P.; Phelps, D. E. *J. Chem. Phys.* **1968**, *48*, 3831–3832.

(43) Levitt, M. H.; Freeman, R. J. *Magn. Reson.* **1981**, *48*, 65–80.

(44) Marion, D.; Wuthrich, K. *Biochem. Biophys. Res. Commun.* **1983**, *113*, 967–974.